Journal of Applied Phycology (2022) 34:2211–2222
https://doi.org/10.1007/s10811-022-02756-5

In vitro antioxidant and anti-glycation properties of *Sargassum horneri* from golden tides on the South Korean coast and the effect on gut microbiota of mice fed a high-sucrose and low-fibre diet

Gayang Lee[1] · Yuko Midorikawa[1] · Takashi Kuda[1] · Mika Harada[1] · Sae Fujita[1] · Hajime Takahashi[1] · Bon Kimura[1]

Received: 26 January 2022 / Revised and accepted: 19 April 2022 / Published online: 13 May 2022

Abstract
Outbreaks of algal blooms for *Sargassum horneri* and *Ulva* spp., called golden and green tides on the South Korean coast, severely damage the local coastal environment and marine ecological system. However, these edible algae are natural resources of beneficial bioactive components, such as dietary fibres, phenolic compounds, and minerals. In this study, the antioxidant and anti-glycation properties of 2% aqueous extract solution (AES) in vitro from *S. horneri* (Sh) and *Ulva pertusa* (Up), and the effects of dried *S. horneri* and Up on the caecal microbiota of mice fed a high-sucrose and low-fiber diet were investigated. Total phenolic content, antioxidant activity (DPPH radical scavenging and Fe-reducing power), and anti-glycation activity in the BSA-fructose model were higher in Sh-AES than in Up-AES groups. Male Institute of Cancer Research (ICR) mice fed a 5% (w/w) *S. horneri* diet for 14 days showed a reduced increase in body weight. 16S rDNA (V4) amplicon sequencing results showed that the ratio of Firmicutes/Bacteroidota was reduced after *S. horneri* and *U. pertusa* intake. *Faecalibaculum rodentium*-, *Akkermansia muciniphila*-, and *Roseburia intestinalis*-like bacteria were enriched in the *S. horneri* group. *Phocaeicola vulgatus*-like bacteria were abundant in both the *S. horneri* and *U. pertusa* groups. In contrast, the prevalence of *Clostridium disporicum*-like bacteria was low in mice fed the *S. horneri* diet. Among the bacteria enriched after *S. horneri* and *U. pertusa* administration, *P. vulgatus* was found to be prevalent. From these results, *S. horneri* from golden tides may be useful as a functional food.

Keywords *Sargassum horneri* · *Ulva pertusa* · Antioxidant · Anti-glycation · Gut microbiome

Introduction

Reports of enormous amounts of floating macroalgal blooms in coastal regions worldwide are increasing every year (van Tussenbroek et al. 2017). Outbreaks of marine algae are known to severely damage the local maritime environment, disrupting the marine ecological system and hindering tourism, aquaculture, and coastal fisheries (Smetacek and Zingone 2013). Although *Sargassum horneri* and *Ulva* spp. are traditionally edible brown and green algae, mass outbreaks have been reported to cause environmental problems along the coast in South Korea (Kim et al. 2018; Song et al. 2018).

Several studies have been conducted on the beneficial compounds that can be obtained from *S. horneri* and *Ulva* spp., such as polysaccharides (alginates, fucoidans, and ulvans), minerals, and phenolic compounds (phlorotannins), prebiotics, antioxidants, and compounds with anti-inflammatory, antiglycation, and anti-cancer activities (Fernando et al. 2018; Seong et al. 2019; Guo et al. 2020; Sanjeewa et al. 2020; Zheng et al. 2020).

High concentrations of reactive oxygen species (ROS) such as OH, O_2^-, and ROO- may disrupt the balance of pro-oxidants/antioxidants in the organism, resulting in oxidative stress which may promote aging and inflammation-related diseases (Pizzino et al. 2017). Various antioxidants have been studied in plant food materials (Amorati and Valgimigli 2018). Phenolic compounds are free radical scavengers, and there are several reports related to phenolic compounds that can help prevent various diseases associated with oxidative stress (Shahidi and Ambigaipalan 2015).

✉ Takashi Kuda
kuda@kaiyodai.ac.jp

[1] Department of Food Science and Technology, Tokyo University of Marine Science and Technology, 4-5-7 Konan, Minato-ku, Tokyo 108-8477, Japan

Glycation is a non-enzymatic reaction that occurs during damage to normal cells and tissue functions in which sulfhydryl protein bonds are replaced by glucose (Yan et al. 2003). Advanced glycation end products (AGEs) produced by glycation contributors to the production of oxidants or induce carbonyl stress, enhance transcriptional factor activity that is sensitive to cellular redox reactions, decrease innate immune defence, and induce inappropriate inflammatory reactions over time (Vlassara 2005). The accumulation of AGEs leads to a variety of diseases, such as aging, diabetes, and cancer (Wei et al. 2018). Several studies have reported that antiglycation capacity is positively linked with the antioxidant activity of polyphenolic compounds (Amorati and Valgimigli 2018; Mizutani et al. 2000).

The human intestine is inhabited by an extremely diverse microbiome containing ~ 100 trillion bacteria which play an important role in human health (Zhang et al. 2010). The gut commensal microbes play a fundamental role in preventing pathogens from entering mucosal tissue and promote homeostatic functions, such as immunomodulation and maintaining barrier function (Quigley 2013). Dietary habits have a significant influence on changes in the gut microbiome composition; in particular, microbe-accessible carbohydrates found in dietary fibre play an important role in shaping the intestinal microbial ecosystem (Sonnenburg et al. 2016). Their metabolites contribute to maintaining the barrier function of the intestines, preventing colorectal cancers, reducing the likelihood of developing obesity, and controlling the mucosal immune system (Shao et al. 2014; Kasubuchi et al. 2015; Yang and Cong 2021).

Although *S. horneri* and *Ulva pertusa* are commercially available as functional food in Japan, the removed *S. horneri* and *U. pertusa* are discarded or used as fertilizer and livestock feed in South Korea. Several studies already have been conducted on the beneficial compounds that can be obtained from *S. horneri* and *Ulva* spp. However, the beneficial effect of *S. horneri* and *U. pertusa* on intestine bacterial community has not been investigated.

In this study, to investigate utility value of *S. horneri* and *U. pertusa* as functional food materials instead of viewing these as causing the problematic golden tides and green tides as mentioned above. We analysed the antioxidant and anti-glycation properties of aqueous extract solutions (AES) from these species. Furthermore, the effect of 5% (w/w) dried *S. horneri* and *U. pertusa* consumption in mice given a high-sucrose and low-fiber diet to alter the intestinal bacteria was evaluated by 16S rRNA gene (V4 region) amplicon sequencing using viable bacteria isolated from the caecum.

Materials and methods

Sample preparation

Sargassum horneri (Sh) from a golden tide on Taeean beach, Republic of Korea, and *Ulva pertusa* (Up) from a green tide on Jeju beach, Republic of Korea, were collected in July 2020. The algal samples were washed three times with tap water to remove salt, sand, and impurities and were subsequently frozen at -80℃. The frozen samples were lyophilised and milled using a grinder to a powder. The milled powders were used for the analysis of algal characteristics and in animal experiments. Distilled water (DW; 2% w/v) was autoclaved at 121 °C for 15 min. The supernatant (AES) was collected after centrifugation at 2500 × *g* for 10 min at 4 °C.

Proximate composition and physicochemical characterization of algal powder

Crude proteins, lipids, ash, and carbohydrates in dried samples were analysed using the AOAC method (AOAC 2006). To determine the saccharide composition, algal samples (10 mg) were mixed with 100 µL 72% H_2SO_4 and hydrolysed at 30℃ for 2 h, followed by the addition of 2.8 mL DW and a second hydrolysis step by autoclaving at 121℃ for 1 h. The monosaccharide composition was analysed using high-performance anion-exchange chromatography with pulsed amperometric detection (HPAEC-PAD, ICS-5000, Dionex, USA) with a CarboPac PA-1 column (250 × 4 mm, Dionex). The gradient elution (18 mmol mL^{-1} NaOH) was performed at 25℃ with a flow rate of 1 mL min^{-1}.

Fourier-transform infrared (FT-IR) spectra of the algae and extract powder were obtained using a Nicolet iS5 FT-IR spectrometer (Thermo Electron Corp., USA) equipped with an IR- attenuated total reflection (ATR) diamond attached. The obtained wavenumber range was 400 to 4000 cm^{-1} at room temperature. The aqueous extract powders (ShE and UpE) were extracted at 90 °C for 2 h using a reflux condenser, and the ethanol extract powders (ShEt and UpEt) were extracted using 70% ethanol overnight at room temperature. The extracted powder samples were freeze-dried.

Analysis of total phenolic content (TPC), antioxidant, and antiglycation activities in AES

TPC was measured using the Folin-Ciocalteu method as described previously (Taniguchi et al. 2021) and expressed as PG equivalents (PGEq) g^{-1} of sample. We evaluated the antioxidant property, DPPH radical scavenging activity, O_2^- radical scavenging activity, and ferric (Fe) reducing power and scavenging activity as described previously (Takei et al. 2017; Harada et al. 2021). The antioxidant capacity was expressed as µmol catechin equivalent (CatEq) mL^{-1}.

Antiglycation activity analysis

The anti-glycation activity in the bovine serum albumin (BSA)-fructose (Fru) and BSA-methylglyoxal (MGO)

models was determined according to a previously described method (Taniguchi et al. 2021). Briefly, 0.5 mL of fructose (1.5 mol L^{-1}), MGO (60 mmol L^{-1}), 0.5 mL of *S. horneri* and *U. pertusa* AESs, and 0.5 mL of sodium phosphate buffer (50 mmol L^{-1}, pH 7.4) containing 0.02% sodium azide were added into each tube. The sample mix was kept at 37 °C for 2 h, and subsequently, 0.5 mL BSA (30 mg mL^{-1}) was added to each tube. The fluorescence intensity (FI) of the mixture was measured immediately using a microplate reader at an excitation/emission wavelength of 340/420 nm (0 days), and the mixture was further incubated at 37 °C for five days. The FI was recorded at the same excitation/emission wavelength after five days. AGE inhibition was calculated using the following formula:

$$Anti-glycation\ activity(\%) = \frac{(1-(FI\ 5\ d\ sample - FI\ 0\ d\ sample)}{(FI\ 5d\ blank - FI\ 0\ d\ blank)} \times 100 \quad (1)$$

Animal care

The animal experiments were designed in accordance with the "Fundamental Guidelines for Proper Conduct of Animal Experiment and Related Activities in Academic Research Institutions" prescribed by the Ministry of Education, Culture, Sports, Science, and Technology, and approved by the Animal Experiment Committee of the Tokyo University of Marine Science and Technology (Approval No. H31-5).

Eighteen 5-week-old male ICR mice were purchased from Tokyo Laboratory Animal Science (Tokyo, Japan) and housed (three mice/cage) under standard laboratory conditions. The mice were adapted to a high-sucrose-low-dietary fibre diet (NF) and were provided distilled water ad libitum for 7 days. The mice were divided into three treatment groups ($n=6$) and fed the no fibre (NF), 5% (w/w) *S. horneri* or 5% *U. pertusa* diets (Table 1) for 14 days. The defaecation frequency and faecal weight were noted from 11 to 13 days during feeding. At the end of the feeding schedule, mice were euthanised after administration of isoflurane (Fujifilm Wako Pure Chemical, Japan), and exsanguinated blood was collected in a 10 µL (10 mg mL^{-1}) heparized tube. The liver, spleen, kidneys, caecum, large intestine, and epididymal fat pads were removed and weighed and the length of the large intestine was measured. The caecum was kept on ice until it was incised for microbiome analysis.

Direct bacterial cell count and isolation

Caecal contents (0.1 g) were diluted with 9.9 mL of phosphate-buffered saline (PBS; Nissui Pharmaceuticals, Japan) and the bacterial cells were counted using dielectrophoretic impedance measurement (DEPIM) (Hirota et al. 2014) with a bacterial counter (PHC Ltd., Japan). To isolate bacteria, 0.03 mL of tenfold dilutions of caecal content containing "dilution A" (KH_2PO_4, 4.5 g; Na_2HPO_4, 6 g; L-cysteine·HCl·H_2O, 0.5 g; Tween 80, 0.5 g; agar, 0.75 g L^{-1}) were spread on blood liver (BL) agar (Nissui Pharmaceuticals) and Gifu Anaerobic Medium (GAM) agar (Nissui Pharmaceuticals) plates; these were subsequently incubated at 37 °C for 48 h under anaerobic conditions using an AnaeroPack (Mitsubishi Gas Chemical, Japan). After incubation, colonies with typical morphology and colour were counted and isolated using the same agar plates. After Gram staining and catalase tests, the 16S rRNA gene from the isolates was amplified using the polymerase chain reaction (PCR) primers 27F and 1492R. Sequencing was performed by Macrogen Japan (Tokyo, Japan), and a homology search was conducted using BLASTn at the National Center for Biotechnology Information (https://blast.ncbi.nlm.nih.gov/Blast.cgi).

Table 1 Consumption of the diet for each feeding group (g (100 g)$^{-1}$)

	NF	5% Sh	5% Up
Sargassum horneri (Sh)		5	
Ulva pertusa (Up)			5
Milk casein	20	20	20
DL-Methionine	0.3	0.3	0.3
Corn starch	20	15	15
Sucrose	50	50	50
Corn oil	5	5	5
Vitamin mix (AIN-76)	1	1	1
Mineral mix (AIN-76)	3.5	3.5	3.5
Choline citartrate	0.2	0.2	0.2

Caecal microbiota analysis using MiSeq

16S rDNA (V4) amplicon sequencing was performed by Fasmac Co., Ltd. (Atsugi, Japan). Briefly, DNA was extracted from the faeces using the MPure bacterial DNA extraction kit (MP Bio Japan, Japan). A DNA library was prepared using a two-step PCR (mentioned above) method (Sinclair et al. 2015). The V4 region was amplified using the primers forward 515f and reverse 806r and ExTaq HS DNA Polymerase (Takara Bio, Japan) for the 1st PCR (94 °C for 2 min, 20 cycles of 94 °C for 30 s, 50 °C for 30 s, 72 °C for 30 s, and a final extension of 72 °C for 5 min). After purification of the PCR products using the AMPure XP kit (Beckman Coulter Life Science, Japan), individual DNA fragments were tagged via a 2nd PCR step (94 °C for 2 min, 8 cycles of 94 °C for 30 s, 60 °C for 30 s, 72 °C for 30 s, and a final extension of 72 °C for 5 min) with the same polymerase kit. DNA libraries were multiplexed and loaded onto the Illumina MiSeq system (Illumina, USA).

Reads with a mismatched sequence at the start region were filtered using the FASTX Toolkit (http://hannonlab.cshl.edu/fastx_toolkit/), and 235–260 base pair reads were

selected. Chimeras were identified and removed using the QIIME2 bioinformatics pipeline (https://qiime2.org/). A feature table was generated using the dada2 denoise-paired option in the QIIME2 plugin (Poncheewin et al. 2020), and the sequences were clustered into amplicon sequence variants (ASVs) using the SILVA 138 database (https://www.arb-silva.de/).

Statistical analysis

Data are expressed as the mean value ± standard error. Analysis of variance followed by Tukey's and Dunnett's post hoc tests were performed using a statistical software package (Excel Statistic Ver. 6, Japan). Statistical significance was set at $P < 0.05$. The alpha diversity (Shannon–Wiener index H, Simpson's index D) of the caecal microbiota was calculated using previously published methods (Kim et al. 2017). To analyse the beta diversity, principal component analysis (PCA) plots based on ASVs were generated using the MetaboAnalyst web service (https://www.metaboanalyst.ca/). To detect typical ASVs in each diet group, linear discriminant analysis effect size (LEfSe) was performed using Galaxy (https://huttenhower.sph.harvard.edu/galaxy/). For functional prediction analysis, PICRUSt was used in combination with the Kyoto Encyclopedia of Genes and Genomes (KEGG) pathway analysis. Taxonomic profiling was performed using the Ez-BioCloud (https://www.ezbiocloud.net/) database.

Results

FT-IR spectra

FT-IR spectra of whole algae (*S. horneri* and *U. pertusa*), aqueous extracts (ShE and UpE), and 70% ethanol extracts (ShE and UpE) are shown in Fig. 1. In the ShEt and UpEt spectra, absorbance bands with peaks at 2850–3000 cm^{-1} and between 1650 and 1760 cm^{-1} were observed. Stretching bands were commonly observed around at 1040, 1420 and 1600 cm^{-1} in the ShE spectrum. In the UpE spectrum, major peaks at 1420 and 1080 cm^{-1} were observed.

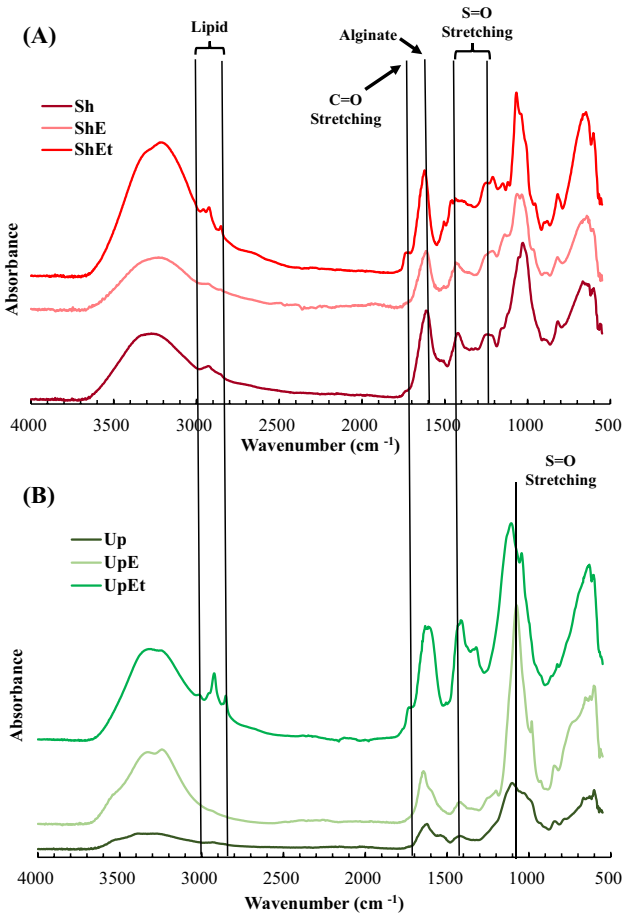

Fig. 1 ATR-FTIR spectra of the dried algal powders from *Sargassum horneri* (**A**) and *Ulva pertusa* (**B**). The terms Sh and Up indicate the profile using dried powders; ShE and UpE indicate aqueous extracts; ShEt and UpEt indicate ethanolic extracts

Proximate and saccharide composition

The proximate and saccharide composition of *S. horneri* and *U. pertusa* are shown in Table 2. The most abundant nutrients were carbohydrates in both *S. horneri* (65%) and *U. pertusa* (59%) groups. Compared to *S. horneri* powder, *U. pertusa* showed a high protein (16%) and lipid (2%) content. Both *S. horneri* (25%) and *U. pertusa* (23%) had a high ash content based on the dry weight. Among the uronic acids in *S. horneri*, mannuronic (94 μg mg^{-1}) and glucuronic acid (8 μg mg^{-1}) were the main compounds of alginate (Kuda et al. 2002). Fucose (29 μg mg^{-1}) and galactose (13 μg mg^{-1}) in *S. horneri* constitute fucoidan (Kuda et al. 2021). *Ulva pertusa* mainly contained rhamnose (116 μg mg^{-1}), xylose (15 μg mg^{-1}), and glucuronic acid (60 μg mg^{-1}) that constitute ulvan (Tako et al. 2015).

TPC and antioxidant properties of aqueous extract solutions

Sh-AES had a high phenolic content of 1 μmol PGEq. mL^{-1}; however, Up-AES was at low levels at 0.1 PGEq. mL^{-1} (Table 2). The DPPH radical scavenging activity of Sh-AES showed a maximum of 16 μmol CatEq. mL^{-1}but was not detected in Up-AES (Fig. 2A). Both AESs showed high O_2^- scavenging activity at 2.7 and 2.3 μmol CatEq. mL^{-1}, respectively. The Fe-reducing power of Sh-AES

Table 2 Nutrients and physicochemical characterization of dried algal powder

	Sargassum horneri (Sh)	*Ulva pertusa* (Up)
Nutrient (%)		
Protein	6.34 ± 0.07	16.42 ± 0.08
Crbohydrate	68.25 ± 0.48	58.73 ± 0.20
Lipid	0.84 ± 0.04	1.96 ± 0.26
Ash	24.57 ± 0.48	22.88 ± 0.04
Monosaccharide composition (μg mg^{-1})		
Fucose	28.63 ± 0.52	ND
Rhamnose	ND	115.99 ± 0.93
Arabinose	ND	ND
Galactose	13.35 ± 0.57	5.56 ± 0.13
Glucose	101.38 ± 0.55	66.35 ± 0.52
Mannose	14.28 ± 1.26	ND
Xylose	4.54 ± 0.55	15.36 ± 0.11
Galacturonic acid	ND	ND
Glucuronic acid	8.14 ± 0.02	60.12 ± 0.84
Mannuronic acid	93.93 ± 1.48	ND
Total polyphenolic acid (phloroglucinol eq. mL^{-1})		
	0.98 ± 0.02	0.06 ± 0.01

Values indicate the mean ± SEM ($n = 3$)

showed a maximum of ~ 18 μmol CatEq. mL^{-1}, and UpE showed reduced Fe-reducing power at 0.6 μmol CatEq. mL^{-1} (Fig. 2C).

Antiglycation capacity

As shown in Fig. 2D, anti-glycation activity in the BSA-Fru model in Sh-AES was high even in the four-fold diluted sample (78%), but it was undetectable in Up-AES. In the MGO-BSA model, Sh-AES and Up-AES showed antiglycation activities levels at ~ 24% and 9%, respectively (Fig. 2E).

Effects on body, faecal, organ weights, and the plasma lipid and glucose levels in mice

Body weight gain during the 14-day feeding period was lower in the Sh group compared with the NF group (Table 3). Defaecation frequency and the faecal wet weight were significantly increased in the Sh and Up groups. Furthermore, the caecal content weight was greater in the Sh groups. Liver weight was low in mice fed Sh, whereas caecal tissue weight was greater in the Sh group. Plasma cholesterol levels were low in the Sh group, although there were no significant differences in plasma lipid and glucose levels compare to NF group.

Effects on the gut microbiome

Direct cell count and diversity analysis

The direct bacterial cell count in the caecal fraction was low in the Sh and Up groups (10.7–10.8 log cells g^{-1}) compared to the NF group (11.4 log cells g^{-1}) (Table 4). The results

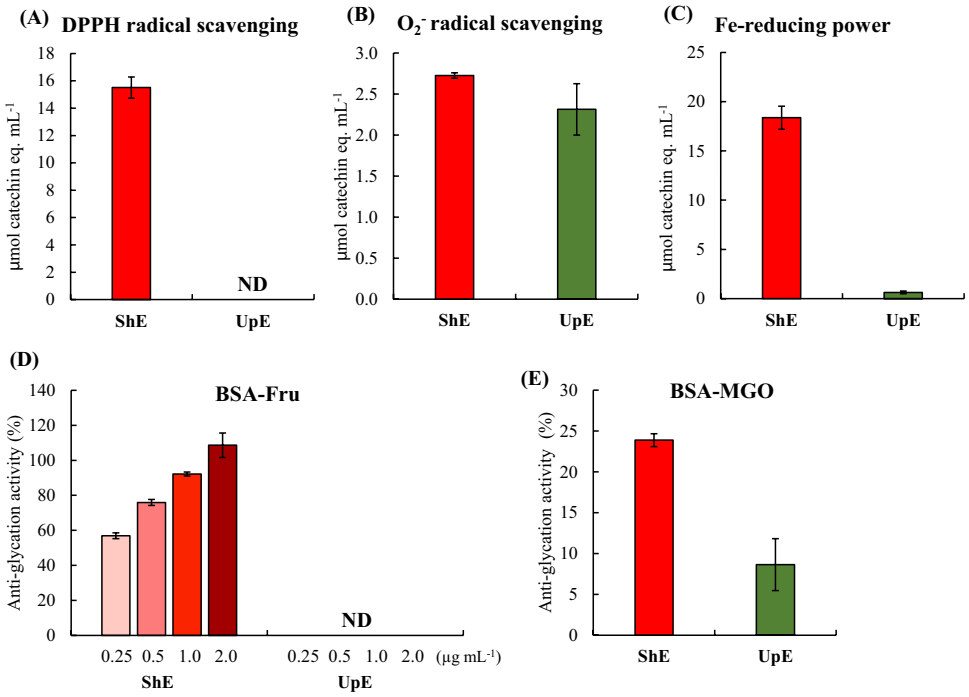

Fig. 2 DPPH radical scavenging (**A**), O_2^- radical scavenging (**B**), Fe-reducing power (**C**), and antiglycation activity in the BSA-fructose model (**D**), and the BSA-methylglyoxal model (**E**) using 2% aqueous extract solutions of Sh and Up. Values indicate the mean ± SEM ($n = 3$).

Table 3 Body, faecal, and organ weights for the no fiber and 5% (w/w) algal diet administered groups

	NF	Sh	Up
Body weight (g)			
Initial	39.0 ± 0.5	38.5 ± 0.8	38.7 ± 0.6
After 14 days	53.7 ± 0.5	49.6 ± 0.7*	53.9 ± 2.0
Gain/14 days	14.8 ± 0.6	11.7 ± 0.9*	17.18 ± 1.3
Defecation			
Frequency (n day^{-1} mouse^{-1})	20 ± 1	47 ± 2*	36 ± 2*
Weight (g day^{-1} mouse^{-1})	0.242 ± 0.010	0.935 ± 0.166*	0.607 ± 0.056*
Caecal content (g)	0.207 ± 0.010	0.309 ± 0.022*	0.273 ± 0.018
Organ weights (g)			
Liver	3.867 ± 0.185	3.099 ± 0.151*	3.525 ± 0.176
Spleen	0.137 ± 0.015	0.122 ± 0.004	0.127 ± 0.010
Kidneys	0.751 ± 0.033	0.658 ± 0.039	0.707 ± 0.035
Caecal wall	0.064 ± 0.005	0.105 ± 0.002*	0.079 ± 0.008
Plasma lipid and glucose levels mg (100 mL)$^{-1}$			
Triacylglycerol	132 ± 20	131 ± 20	131 ± 18
Total cholesterol	204 ± 16	178 ± 9	203 ± 15
Glucose	486 ± 33	478 ± 22	541 ± 56

Values are shown as the mean ± SEM ($n = 6$)

*Significant difference relative to the NF group using Dunnett's test ($p < 0.05$)

from the 16S rDNA(V4) sequencing yielded a total read number of 105,000–122,000. The number of ASV types and the values of the α-diversity indices, i.e., Shannon–Wiener index (H') and Simpson's index (D) were significantly greater in the Up group (Table 4). The PCA plot of ASVs (Fig. 3A and B) showed that the gut microbiota composition differed among the diet-based groups.

Phylum, family, and genus characterization

The abundance of the caecal microbes at the phylum, family, and genus levels is shown in Fig. 3C-F. The most abundant phylum in the NF group was Firmicutes (77%), followed by Actinobacteria (20%), Bacteroidota (2.3%), and Desulfobacterota (1.1%). The abundance of Bacteroidota was significantly greater in the Sh (20%) and Up (16%) groups than in the NF group. The Firmicutes/Bacteroidota (F/B) ratio was considerably reduced after algal consumption compared to the NF diet group. Verrucomicrobiota enrichment was high in the Sh group (6%), whereas Actinobacteria abundance was low in the Sh group.

In the phylum Firmicutes, *Erysipelotrichaceae* (36.6%), *Clostridiaceae* (25%), *Lactobacillaceae* (4.3%), and *Lachnospiraceae* (6.8%) were the dominant families in the NF group. *Clostridiaceae* abundance was significantly reduced in the Sh group (0.06%). For Bacteroidota in the Sh and Up groups, *Bacteroidaceae* and *Muribaculacceae* were the dominant families. The dominant family of Verrucomicrobiota in the Sh group was *Akkermansiaceae*. The dominant family in Actinobacteria was *Bifidobacteriaceae*. The dominant genera from the family *Erysipelotrichaceae* were *Faecalibaculum* (16.8%) and *Allobaculum* (16%) in the NF group, whereas these genera showed high (36%) and low (5%), levels, respectively, in the Sh group. Most *Clostridiaceae* species were identified as *Clostridium* sensu_stricto_1.

Table 4 Caecal bacterial cell count and α-diversity of the caecal microbiome showing differences between the no fiber and 5% algae groups

	NF	Sh	Up
Bacterial count (Log cells/g)	11.37 ± 0.10	10.78 ± 0.16*	10.70 ± 0.11*
16S rRNA gene amplicon sequencing			
Total read number	107,082 ± 4207	121,941 ± 5941	105,115 ± 4653
Number of ASVs	184 ± 12	179 ± 4	285 ± 6*
Shannon–Weaver H'	2.582 ± 0.102	2.883 ± 0.218	3.531 ± 0.117*
Shimpson's index (D)	0.861 ± 0.012	0.831 ± 0.033	0.930 ± 0.010*

Values are shown as the mean ± SEM ($n = 5$)

*Significant difference relative to the NF group using Dunnett's test ($p < 0.05$)

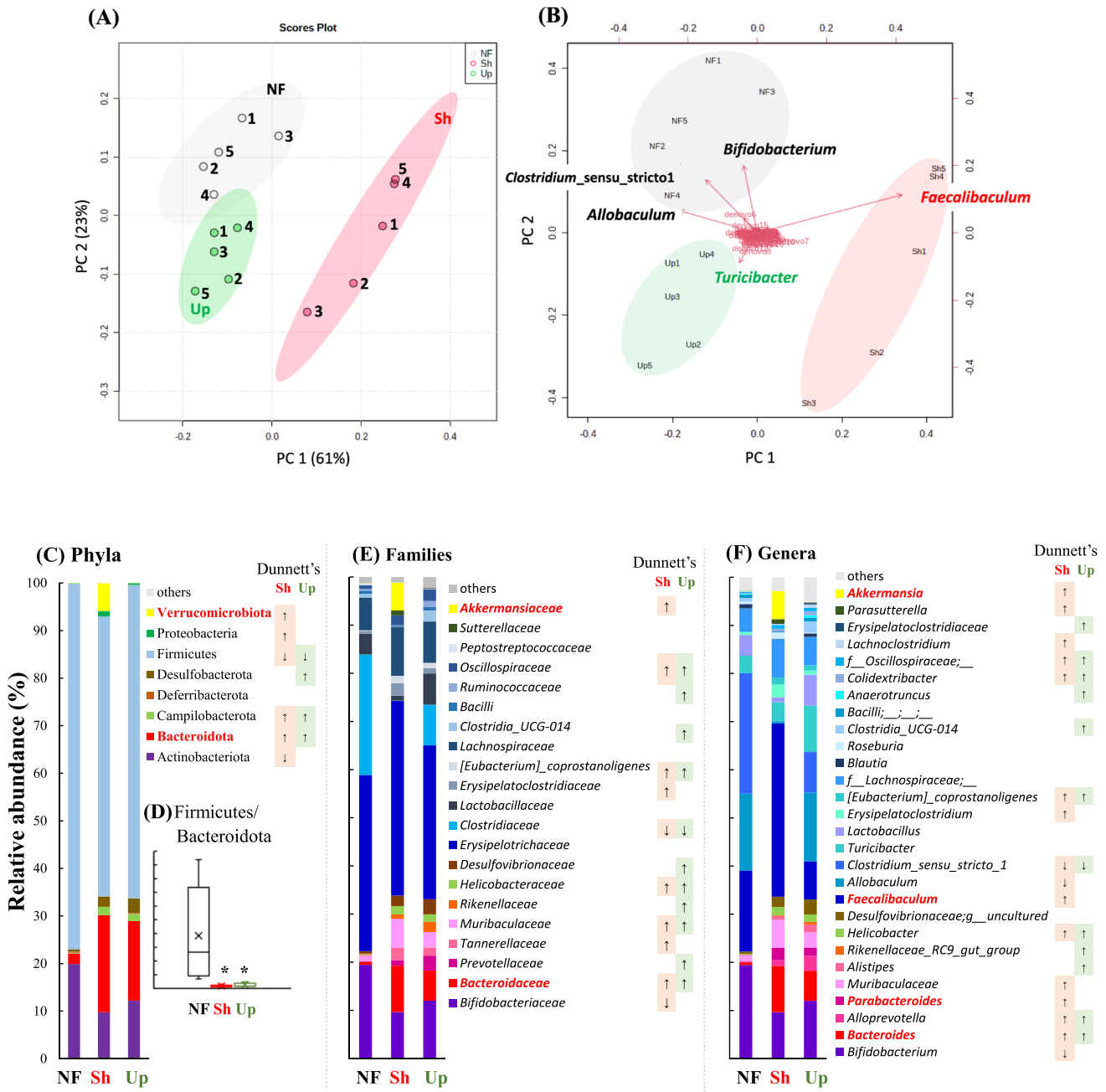

Fig. 3 Principal component analysis (PCA; **A**), PCA biplot based on ASV level (**B**), enrichment at phylum (**C**), family (**E**), and genus (**F**) levels in caecal microbiota of mice fed a high-sucrose and low-fibre diet containing no fibre (NF), 5% (w/w) dried *Sargassum horneri* (Sh) and *Ulva pertusa* (Up). (**D**) The Firmicutes/Bacteroidota ratio (F/B). Significant differences relative to the NF group using Dunnett's test (↑↓ $p < 0.05$). *Significant different relative to the NF group using Dunnett's test ($p < 0.05$)

ASV level

The taxonomic cladogram and LDA score (Fig. 4A) results indicated that *Clostridia*_UCG_014 in the NF group was significantly lower after consumption of the Sh diet. Moreover, the enrichment of *Akkermansia* spp., *Faecalibaculum* spp., *Roseburia* spp., and *Parabacteroides* spp. was high in the Sh group. The ASV heat map (Fig. 4B, Table S1) showed that *Akkermansia muciniphila* (similarity 100%), *Roseburia intestinalis* (100%), and *Faecalibaculum rodentoum* (100%)-like bacteria were typical of the Sh group. Conversely, several *Clostridium* ASVs, such as *C. disporicum/saudiense* and *Allobaculum* sp.-like bacteria were significantly affected by algal consumption in the Sh group. ASVs in Bacteroidota

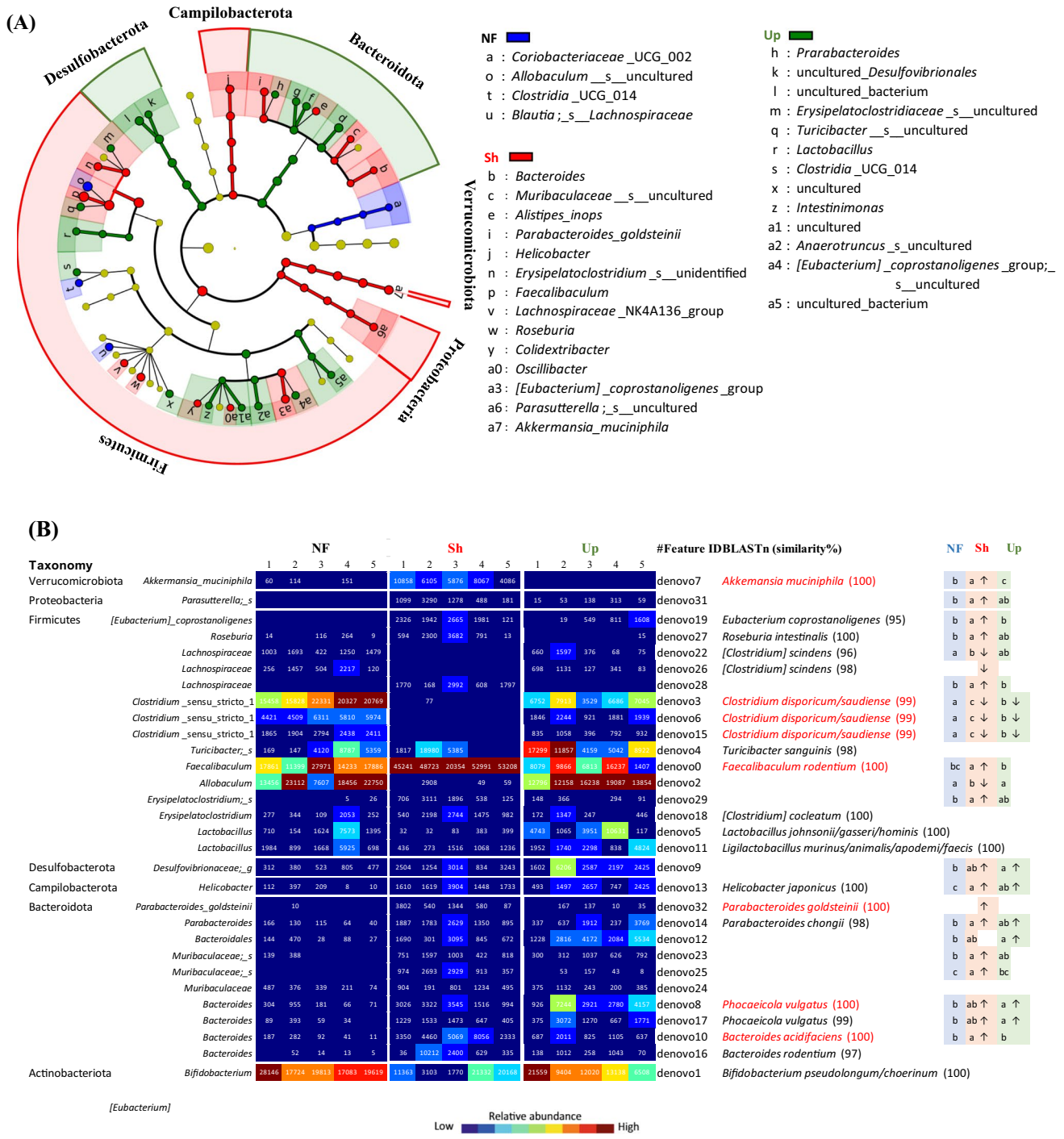

Fig. 4 Based on the ASV level of caecum bacteria communities, Linear discriminant analysis (LDA) effect size taxonomic cladogram (**A**), and heat map analysis of the top 30 selected abundant ASVs (**B**) in caecal microbiota of mice fed a high-sucrose and low-fibre diet containing no fibre (NF), 5% (w/w) dried *Sargassum horneri* (Sh) and *Ulva pertusa* (Up) are shown. $^{a-c}$ Values with different alphabet letters indicate significant differences identified using Tukey's test at $p < 0.05$. Significant difference relative to the NF group using Dunnett's test (↑↓, $p < 0.05$)

that were high in the Sh and Up group were identified as *Phocaeicola vulgatus* (100%)-like bacteria. *Parabacteroides goldsteinii* (100%)-, and *Bacteroides acidifaciens* (100%)-like bacteria were enriched in the Sh group. Among the typical bacterial species, *P. vulgatus* (accession numbers: LC645986, LC645990) and *P. goldsteinii* (LC645989) were isolated from BL and GAM agar plates.

Predictive gut microbiome functional biomarkers

LEfSe analysis was performed to identify the relevant functional pathways associated with the differences between the NF and the *S. horneri* diet groups (Fig. 5). The "Other glycan degradation (ko00511)" and "Lipopolysaccharide biosynthesis (ko00540)" were significantly increased by *S. horneri* intake, whereas "Starch and sucrose metabolism (ko00500)" was decreased compared with the NF group.

Discussion

As mentioned above, large amounts of *S. horneri* and *U. pertusa* tides on the coasts in South Korea are problematic for fisheries and the environment (Kim et al. 2018; Song et al. 2018). In this study we attempted to utilise algae from these golden and green tides as a useful resource, and reduce the burden on industry and the environment. We examined the in vitro antioxidant levels, anti-glycation effects, and the effects on mice fed a high-sucrose and low-fiber diet. Base on the FTIR analysis, several compounds were determined (Fig. 1). The absorbance peaks between 2850 and 3000 cm^{-1} indicate the presence of lipid, and peaks between 1650 and 1760 cm^{-1} indicate the C = O group stretching vibration in carbonyl compounds such as carboxylic acids, esters, ketones, and aldehydes in the ShEt and UpEt spectra (Laurens and Wolfrum 2011; Nunes et al. 2019). In the ShE and UpE spectrum, the peaks at 1420 and 1250 cm^{-1} indicate S = O stretching as a sulfate group (Jesumani et al. 2019; Sanjeewa et al. 2020). Moreover, the peak at 1600 cm^{-1} indicates the presence of alginate in ShE (Mohammed et al. 2018). In UpE, the peak at 1070 cm^{-1} represents the stretching vibration of S = O suggesting that sulfate groups

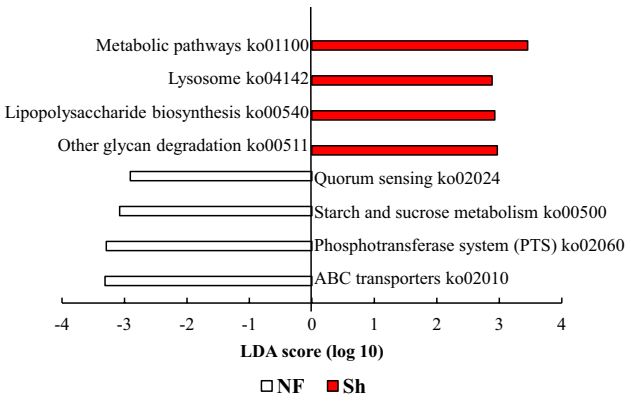

Fig. 5 Differences in the pathway profiles using Kyoto Encyclopedia of Genes and Genomes (KEGG) analysis modified by LEfSe ($p < 0.01$) for caecal microbiota in mice fed a high sucrose-containing diet with no fibre ($n = 5$) and 5% (w/w) *Sargassum horneri* ($n = 5$)

(Peasura et al. 2015). Based on the nutrient analysis, it was determined that the both algae had the highest carbohydrate content, more than 50% (Table 1). Both algae had the highest content of glucose, which constitutes cellulose (Table 1). In addition, galactose and fucose, which constitute fucoidan (Kuda et al. 2021), and mannuronic and glucuronic acid, which make up alginate (Kuda et al. 2002), were contained. Followed by FTIR and monosaccharide analysis, it has become clear that both algae contain mainly bioactive polysaccharide such as fucoidan, alginate, and ulvan. According to previous report, it is known that not only the nutrient compounds, but also alginate and fucoidan in Sh, change with season (Murakami et al. 2011).

Several havestudies reported that active oxygen produced by oxidation reactions causes cell degeneration in vivo, which can lead to chronic diseases in humans. Therefore, studies are being conducted on antioxidant components derived from food to suppress oxidative damage to the human body. Therefore, antioxidant activity of the water-soluble compounds in both algae were investigated (Table 2 and Fig. 2A-C). Sh-AES showed high levels of TPC and antioxidant activity. High levels of TPC is beneficial for human health and is abundant in several species of marine algae, especially in brown algae compared to red and green algae (Lv et al. 2014). Among the bioactive compounds present in brown algae, phlorotannin has strong antioxidant activity (Takei et al. 2017). There is a positive correlation between TPC and DPPH radical scavenging and Fe-reducing activities, but not the O_2^- radical scavenging activity. The effects of high O_2^- radical scavenging activity in both AESs may result due to sulphated polysaccharides contained in *S. horneri* and *U. pertusa* (Kuda et al. 2021). In addition, it has been reported that the enhanced radical scavenging activity of sulphated polysaccharides relative to the neutral form may result due to the inhibition of radical generation by chelating ions such as Fe^{2+} and Cu^{2+}, or the role of the sulfate group as an electrophile which promotes intramolecular hydrogen abstraction (Shao et al. 2013). There are some reports on high TPC and antioxidant properties in Sh-AES (Shao et al. 2014; Kuda et al. 2021).

As mentioned above, accumulation of AGE through glycation activity causes various diseases such as aging, diabetes, and cancer (Wei et al. 2018). Therefore, suppressing AGEs generation is an important task. The carbonyl group of sugar and the amino group of proteins produces Amadori products through the Maillard reaction (Zhao et al. 2021). The Amadori products form reactive intermediate dicarbonyls such as methylglyoxal (MGO), glyoxal, and 3-deoxyglucosame, which contribute to AGE generation (Wang et al. 2011). In particular, since fructose and fructose metabolites located in cells participate in glycation reactions at a much faster rate than glucose (Schalkwijk et al. 2004). In the BSA-Fru model, Sh-AES shown high anti-glycation activity even in

the four-fold diluted sample as 78% (Fig. 2E). The BSA-Fru model is a glycation-imitation model for identifying the inhibition rate of AGE and intermediate product formation due to the reaction between a free amino acid group and sugar under hyperglycaemic conditions (Guo et al. 2020). Therefore, the high anti-glycation activity of Sh-AES in the BSA-Fru model indicates that the formation of various intermediate products and AGEs can be suppressed by components present in Sh-AES (Park and Lee 2021). A previous study showed a positive correlation between the anti-glycation effect and the saccharide composition of each extract in the BSA-Fru model in *Ecklonia cava* extracts based on the extraction method (Park and Lee 2021). Therefore, it is expected that the high glycation inhibitory activity of the Sh-AES results due to the TPC and the sulphated polysaccharides. Although Sh-AES showed high anti-glycation activity (BSA-Fru model) in our study, it was low in previous study (Eda et al. 2016). It is expected that these antioxidant and anti-glycation activities were affected by changes in Sh nutrient composition due to seasonal changes (Murakami et al. 2011).

To determine the dietary effects of *S. horneri* and *U. pertusa*, a high-sucrose diet containing no dietary fibre (NF), 5% *S. horneri* and *U. pertusa* was adapted to ICR mice for 14 days. As shown in Table 3, compared with those in mice fed NF, body weight gain and liver weight were lower in mice fed *S. horneri* with higher defaecation frequency, caecal content and tissue weight. The increase in defaecation and caecal content may result due to the presence of insoluble fibres such as cellulose, and water-conjugating polysaccharides such as alginate (Takei et al. 2020). In addition, the increase in caecal tissue weight may result because of epithelial cell proliferation due to the increase in SCFAs (Knapp et al. 2013). Changes in liver weight are associated with inhibition of liver fat accumulation. No fibre group consumed a high-sucrose diet, and high carbohydrate make fatty liver with increases the TG in the liver (Duwaerts and Maher 2019). *Akkermansia muciniphila*, increased by algae consumption, is degraded mucin to propionate and propionate is able to reduce liver fat (Ottman et al. 2017; Duwaerts and Maher 2019). According to previous report, appear of both de novo lipogenesis (DNL) and cholesterogenesis in the liver are to be inhibited by propionate (Morrison and Preston 2016). The bacterial cell count and α-diversity were higher in Up group than NF group (Table 4). Caecal bacterial cells may be diluted by the dietary fibre from *S. horneri* and *U. pertusa* which are includinced in the caecal content weight (Table 2). Consequently, the α-diversity for the Up group is in agreement with a previous report showing that the alpha diversity of the high dietary fibre intake group was greater relative to the low dietary fibre group (Sonnenburg et al. 2016; Takei et al. 2019).

The alteration of caecal bacteria composition was shown in Figs. 3 and 4. Several studies have reported that a high sucrose diet leads to increased Firmicutes and decreased Bacteroidota abundance, and the F/B ratio was positively related to obesity (Kong et al. 2019). The enrichment of *S. horneri* at the phylum level Bacteroidota was similar to previous results using the brown alga *Eisenia bicyclis* and for low molecular weight alginate and laminaran-fed mice at the family level for bacteria enriched in the caecum (Takei et al. 2019, 2020). Bacteroidota contains species that can degrade algal polysaccharides and produce short-chain fatty acids (SCFAs) and other organic acids (Takei et al. 2020; Zheng et al. 2020). The presence of *Clostridium* sensu_stricto_1, which indicates a high risk of infectious diseases, was suppressed by *S. horneri* and Up consumption (Chi et al. 2020). *A. muciniphila* degrades mucin to produce acetate, propionate, and 1,2-propanediol, and attracts microbial species that stimulate the health of the host by preventing the generation of butyrate and pathogenic microbial colonisation (Ottman et al. 2017). The presence of the butyrate-producing genus *Roseburia* reportedly shows beneficial effects. For example, *R. intestinalis* increases Treg cells in the large intestine which is inhibited during intestinal inflammation, and increases immunity by promoting the secretion of TSLP and TGF-β from epithelial cells (Shen et al. 2018). *Parabacteroides goldsteinii* and *B. acidifaciens* are associated with metabolic diseases such as diabetes and obesity (Yang et al. 2017; Wu et al. 2019). As shown in Fig. 5, four functional pathways in caecal bacteria were differentially relevant in the Sh group compare to NF group. Among the abundant functional pathway, "Lipopolysaccharide biosynthesis (ko00540)" genes were associated with the Fusobacteria, Bacteroidota, and Proteobacteria phyla and genes associated with "other glycan degradation (ko00511)" are abundant in the Bacteroidota (Zou et al. 2019).

The results of this study showed that consumption of both *S. horneri* and *U. pertusa* have beneficial effects, such as providing strong O_2^- radical scavenging capacity and dietary fibre in mice. The effects of indigenous bacteria in the gut including *Bacteroides* sp., *Parabacteroides* sp., and *Phocaeicola* sp were promoted by consumption of *S. horneri* and *U. pertusa*. Furthermore, *S. horneri* consumption induced DPPH radical scavenging, showed Fe-reducing power, and had an inhibitory effect on BSA-Fru model glycation. Additionally, Sh consumption may increase the prevalence of positively-acting gut commensals, such as *A. muciniphila* and *Roseburia* sp. These results suggest that algal beach blooms, particularly from golden tides, can be a useful resource for humans and livestock if they can be recovered before decomposition. The synergistic food functionality of *S. horneri* and *S. horneri* -responsive bacteria will be the subject of future studies.

Conclusions

The algal extracts showed high antioxidant TPC, DPPH, and Fe-reducing power. The O_2^- scavenging activity was high in the *S. horneri*—and Up AESs. In addition, Sh-AES showed

higher anti-glycation activity in the BSA-fru model. Compared with the NF group, body and liver weights were significantly reduced in the Sh group. Defaecation frequency and faecal weight in mice fed a high-sucrose and low-fibre diet were significantly increased after intake of either *S. horneri* or *U. pertusa*. The ratio of Firmicutes/Bacteroidota in the caecal content was decreased after either *S. horneri* or Up consumption. *P. vulgatus*-like bacteria were abundant in the Sh and Up groups. In addition, *F. rodentium, A. muciniphila,* and *R. intestinalis*-like bacteria were high in mice fed with *S. horneri*. In contrast, *C. disporicum*-like bacteria were significantly reduced after consumption of the *S. horneri* diet. These results suggest that *S. horneri* has antioxidant and anti-glycation properties, is a rich natural source of dietary fiber, and may be useful for improving health.

Supplementary Information The online version contains supplementary material available at https://doi.org/10.1007/s10811-022-02756-5.

Acknowledgements This work was partially supported by the Yanmar Resource Recycling Support Organization, Tokyo, Japan and the Toyo Suisan Foundation, Tokyo, Japan. The authors thank Editage (www.editage.com) for their assistance with English language editing.

Author contribution Gayang Lee: conceptualisation, methodology, validation, formal analysis, investigation, resources, data curation, writing – original draft, visualisation. Yuko Midorikawa: conceptualisation, methodology, validation, formal analysis, investigation. Takashi Kuda: Conceptualisation, methodology, validation, formal analysis, resources, data curation, writing – review and editing, visualisation, supervision, project administration. Mika Harada and Sae Fujita: formal analysis and investigation. Hajime Takahashi: Conceptualisation, Methodology, Supervision. Bon Kimura: Conceptualisation and supervision.

Data availability The datasets generated during and/or analysed during the current study are available from the corresponding author on reasonable request.

Declarations

Competing interest The authors declare that they have no known competing financial interests or personal relationships that could have influenced the work reported in this paper.

References

Amorati A, Valgimigli L (2018) Methods to measure the antioxidant activity of phytochemicals and plant extracts. J Agric Food Chem 66:3324–3329

AOAC Intl (2006) Official methods of analysis, 18th ed. Association of Official Analytical Chemists (AOAC). Washington, DC

Chi C, Xue Y, Liu R, Wang Y, Lv N, Zeng H, Buys N, Zhu B, Sun J, Yin C et al (2020) Effects of a formula with a probiotic *Bifidobacterium lactis* supplement on the gut microbiota of low birth weight infants. Eur J Nutr 59:1493–1503

Duwaerts CC, Maher JJ (2019) Macronutrients and the adipose-liver axis in obesity and fatty liver. Cell Mol Gastroenterol Hepatol 7:749–761

Eda M, Kuda T, Kataoka M, Takahashi H, Kimura B (2016) Anti-glycation properties of the aqueous extract solutions of dried algae products harvested and made in the Miura Peninsula, Japan, and effect of lactic acid fermentation on the properties. J Appl Phycol 28:3617–3624

Fernando IPS, Jayawardena TU, Sanjeewa KKA, Wang L, Jeon YJ, Lee WW (2018) Anti-inflammatory potential of alginic acid from *Sargassum horneri* against urban aerosol-induced inflammatory responses in keratinocytes and macrophages. Ecotoxicol Environ Saf 160:24–31

Guo L, Goff HD, Xu F, Liu F, Ma J, Chen M, Zhong F (2020) The effect of sodium alginate on nutrient digestion and metabolic responses during both in vitro and in vivo digestion process. Food Hydrocolloids 107:105304

Harada M, Kuda T, Nakamura S, Lee GY, Hajime T, Kimura B (2021) *In vitro* antioxidant and immunomodulation capacities of low-molecular weight-alginate- and laminaran-responsible gut indigenous bacteria. LWT Food Sci Technol 151:112127

Hirota K, Inagaki S, Hamada R, Ishihara K, Miyake Y (2014) Evaluation of a rapid oral bacteria quantification system using dielectrophoresis and the impedance measurement. Biocontrol Sci 19:45–49

Jesumani V, Du H, Pei O, Zheng C, Cheong KL, Huang N (2019) Unravelling property of polysaccharides from *Sargassum* sp. as an anti-wrinkle and skin whitening property. Int J Biol Macromol 140:216–224

Kasubuchi M, Hasegawa S, Hiramatsu T, Ichimura A, Kimura I (2015) Dietary gut microbial metabolites, short-chain fatty acids, and host metabolic regulation. Nutrients 7:2839–2849

Kim HS, Sanjeewa KKA, Fernando IPS, Ryu BM, Yang HW, Ahn G, Kang MC, Heo SJ, Je JG, Jeon YJ (2018) A comparative study of *Sargassum horneri* Korea and China strains collected along the coast of Jeju island South Korea: Its components and bioactive properties. Algae 33:341–349

Kim BR, Shin J, Guevarra RB, Lee JH, Kim DW, Seol JH, Lee JH, Kim HB, Isaacson R (2017) Deciphering diversity indices for a better understanding of microbial communities. J Microbiol Biotechnol 27:2089–2093

Knapp BK, Bauer LL, Swanson KS, Swanson KS, Tappenden KA, Fahey JRGC, Godoy MRC (2013) Soluble fiber dextrin and soluble corn fiber supplementation modify indices of health in cecum and colon of Sprague-Dawley rats. Nutrients 5:396–410

Kong C, Gao R, Yan X, Huang L, Qin H (2019) Probiotics improve gut microbiota dysbiosis in obese mice fed a high-fat or high-sucrose diet. Nutrition 60:175–184

Kuda T, Nishizawa M, Toshima D, Matsushima K, Yoshida S, Takahashi H, Kimura B, Yamagishi T (2021) Antioxidant and anti-norovirus properties of aqueous acetic acid macromolecular extracts of edible brown macroalgae. LWT Food Sci Technol 141:110942

Kuda T, Taniguchi E, Nishizawa M, Araki Y (2002) Fate of water-soluble polysaccharides in dried *Chorda filum* a brown alga during water washing. J Food Compos Anal 15:3–9

Laurens LML, Wolfrum EJ (2011) Feasibility of spectroscopic characterization of algal lipids: Chemometric correlation of NIR and FTIR spectra with exogenous lipids in algal biomass. Bioenergy Res 4:22–35

Lv L, Cheng Y, Zheng T, Li X, Zhai R (2014) Purification, antioxidant activity and antiglycation of polysaccharides from *Polygonum multiflorum* Thunb. Carbohyd Polym 99:765–773

Mohammed A, Bissoon R, Bajnath E, Mohammaed K, Lee T, Bissram M, John N, Kjalsa N, Lee KY, Ward K (2018) Multistage extraction and purification of waste *Sargassum natans* to produce sodium alginate: An optimization approach. Carbohyd Polym 198:109–118

Morrison DJ, Preston T (2016) Formation of short chain fatty acids by the gut microbiota and their impact on human metabolism. Gut Microbes 7:189–200

Mizutani K, Ikeda K, Yamori Y (2000) Resveratrol inhibits AGEs-induced proliferation and collagen synthesis activity in vascular smooth muscle cells from stroke-prone spontaneously hypertensive rats. Biochem Biophys Res Commun 274:61–67

Murakami K, Yamaguchi Y, Noda K, Fujii T, Shinohara N, Ushirokawa T et al (2011) Seasonal variation in the chemical composition of a marine brown alga, *Sargassum horneri* (Turner) C. Agardh. J Food Compos Anal 24:231–236

Nunes N, Rosa GP, Ferraz S, Barreto MC, Pinheiro de Carvalho MAA (2019) Fatty acid composition, TLC screening, ATR-FTIR analysis, anti-cholinesterase activity, and in vitro cytotoxicity to A549 tumor cell line of extracts of 3 macroalgae collected in Madeira. J Appl Phycol 32:759–771

Ottman N, Geerlings SY, Aalvink S, Vos WM, Belzer C et al (2017) Action and function of *Akkermansia muciniphila* in microbiome ecology, health and disease. Best Pract Res Clin Gastroenterol 31:637–642

Park JJ, Lee WY (2021) Anti-glycation effect of *Ecklonia cava* polysaccharides extracted by combined ultrasound and enzyme-assisted extraction. Int J Biol Macromol 180:684–691

Peasura N, Laohakunjit N, Kerdchoechuen O, Wanlapa S (2015) Characteristics and antioxidant of *Ulva intestinalis* sulphated polysaccharides extracted with different solvents. Int J Biol Macromol 81:912–919

Pizzino G, Irrera N, Cucinotta M, Pallio G, Mannino F, Arcoraci V et al (2017) Oxidative stress: Harms and benefits for human health. Oxid Med Cell Longev 2017:841676313

Poncheewin W, Hermes GDA, van Dam JCJ, Koehorst JJ, Smidt H, Schaap PJ (2020) NG-Tax 2.0: A Semantic framework for high-throughput amplicon analysis. Front Genet 10:1366

Quigley EMM (2013) Gut bacteria in health and disease. Gastroenterol Hepatol 9:560–569

Sanjeewa KKA, Jayawardena TU, Kim SY, Lee HG, Je JG, Jee Y, Jeon YJ (2020) *Sargassum horneri* (Turner) inhibit urban particulate matter-induced inflammation in MH-S lung macrophages via blocking TLRs mediated NF-κB and MAPK activation. J Ethnopharmacol 249:112363

Schalkwijk CG, Stehouwer CDA, van Hinsbergh VWM (2004) Fructose-mediated non-enzymatic glycation: sweet coupling or bad modification. Diabetes Metab Res Rev 20:369–382

Seong H, Bae JH, Seo JS, Seo JS, Kim SA, Kim TJ, Han NS (2019) Comparative analysis of prebiotic effects of seaweed polysaccharides laminaran, porphyran, and ulvan using in vitro human fecal fermentation. J Funct Foods 57:408–416

Shahidi F, Ambigaipalan P (2015) Phenolics and polyphenolics in foods, beverages and spices: Antioxidant activity and health effects – A review. J Funct Foods 18:820–897

Shao P, Chen X, Sun P (2013) In vitro antioxidant and antitumor activities of different sulfated polysaccharides isolated from three algae. Int J Biol Macromol 62:155–161

Shao P, Chen X, Sun P, Sun P (2014) Chemical characterization, antioxidant and antitumor activity of sulfated polysaccharide from *Sargassum horneri*. Carbohyd Polym 105:260–269

Shen Z, Zhu C, Quan Y, Yang J, Yuan W, Yang Z, Wu S, Luo W, Tan B, Wang X (2018) Insights into *Roseburia intestinalis* which alleviates experimental colitis pathology by inducing anti-inflammatory responses. J Gastroenterol Hepatol 33:1751–1760

Sinclair L, Osman OA, Bertilsson S, Eiler A (2015) Microbial community composition and diversity via 16S rRNA gene amplicons: Evaluating the illumina platform. PLoS ONE 10:e0116955

Smetacek V, Zingone A (2013) Green and golden seaweed tides on the rise. Nature 504:84–88

Song W, Wang Z, Zhang X, Li Y (2018) Ethanol extract from *Ulva prolifera* prevents high-fat diet-induced insulin resistance, oxidative stress, and inflammation response in mice. Biomed Res Int 9:1374565

Sonnenburg ED, Smits SA, Tikhonov M, Higginbottom SH, Wingreen NS, Sonnenburg JL (2016) Diet-induced extinctions in the gut microbiota compound over generations. Nature 529:212–215

Takei M, Kuda T, Eda M, Shikano A, Takahashi H, Kimura B (2017) Antioxidant and fermentation properties of aqueous solutions of dried algal products from the Boso Peninsula, Japan. Food Biosci 19:85–91

Takei M, Kuda T, Fukunaga M, Toyama A, Goto M, Takahashi H et al (2019) Effects of edible algae on caecal microbiomes of ICR mice fed a high-sucrose and low–dietary fibre diet. JAppl Phycol 31:3696–3978

Takei MN, Kuda T, Taniguchi M, Nakamura S, Takahashi T, Kimura B (2020) Detection and isolation of low molecular weight alginate- and laminaransusceptible gut indigenous bacteria from ICR mice. Carbohyd Polymers 238:116205

Tako M, Tamanaha M, Tamashiro Y, Uechi S (2015) Structure of ulvan isolated from the edible green seaweed, *Ulva pertusa*. Adv Biosci Biotechnol 6:60824

Taniguchi M, Kuda T, Takei M, Takahashi H, Kimura B (2021) Effects of fermented *Aphanizomenon flos-aquae* on the caecal microbiome of mice fed a high-sucrose and low-dietary fibre diet. J Appl Phycol 33:397–407

van Tussenbroek BI, Hernández AHA, Rodríguez-Martínez RE, Julio Espinoza-Avalosb HM, Canizales-Floresa CE, González-Godoy CE (2017) Severe impacts of brown tides caused by *Sargassum* spp. on near-shore Caribbean seagrass communities. Mar Pollut Bull 122:272–281

Vlassara H (2005) Advanced glycation in health and disease: Role of the modern environment. Ann N Y Acad Sci 1043:452–460

Wang W, Yagiz Y, Buran TJ, Nunes CdN, Gu L (2011) Phytochemicals from berries and grapes inhibited the formation of advanced glycation end-products by scavenging reactive carbonyls. Food Res Int 44:2666–2673

Wei Q, Liu T, Sun DW, Sun DS (2018) Advanced glycation end-products (AGEs) in foods and their detecting techniques and methods: A review. Trends Food Sci Technol 82:32–45

Wu TR, Lin CS, Chang CJ, Lin TL, Martel J, Ko YF, Ojcius DM, Lu CC, Young JD, Lai HC (2019) Gut commensal *Parabacteroides goldsteinii* plays a predominant role in the anti-obesity effects of polysaccharides isolated from *Hirsutella sinensis*. Gut 68:248–262

Yan SF, Ramasamy R, Naka Y, Schmidt AM (2003) Glycation, inflammation, and RAGE: a scaffold for the macrovascular complications of diabetes and beyond. Circulation Res 93:1159–11

Yang JY, Lee YS, Kim Y, Lee SH, Ryu S, Fukuda S, et al. (2017) Gut commensal *Bacteroides acidifaciens* prevents obesity and improves insulin sensitivity in mice. Mucosal Immunol 10:104–116

Yang W, Cong Y (2021) Gut microbiota-derived metabolites in the regulation of host immune responses and immune-related inflammatory diseases. Cell Mol Immunol 18:866–877

Zhao L, Zhu X, Yu Y, He L, Li Y, Liu R (2021) Comprehensive analysis of the anti-glycation effect of peanut skin extract. Food Chem 362:130169

Zhang Z, Wang F, Wang X, Liu X, Hou Y, Zhang Q (2010) Extraction of the polysaccharides from five algae and their potential antioxidant activity in vitro. Carbohyd Polym 82:118–121

Zheng LX, Chen XQ, Cheong KL (2020) Current trends in marine algae polysaccharides: The digestive tract, microbial catabolism, and prebiotic potential. Int J Biol Macromol 151:344–354

Zou Y, Xue W, Luo G, Deong Z, Qin P, Guo R et al (2019) 1,520 reference genomes from cultivated human gut bacteria enable functional microbiome analyses. Nat Biotechnol 37:179–185